Hydrophilic interaction liquid chromatography-tandem mass spectrometry for the quantitative analysis of mammalian-derived inositol poly/pyrophosphates

Masatoshi Ito[1], Natsuko Fujii[2], Christopher Wittwer[3], Ayumi Sasaki[1], Masayuki Tanaka[1], Tamara Bittner[3], Henning J. Jessen[3], Adolfo Saiardi[4], Shunya Takizawa[2], Eiichiro Nagata[2]

[1]Support Center for Medical Research and Education, [2]Department of Neurology, Tokai University School of Medicine, Kanagawa 259-1193, Japan, [3]Institute of Organic Chemistry, University of Freiburg, 79104 Freiburg, Germany, [4]Cell Biology Unit, Medical Research Council Laboratory for Molecular Cell Biology, and Department of Cell and Developmental Biology, University College London, WC1E 6BT, United Kingdom.

Corresponding to: Eiichiro Nagata, M.D., Ph.D.
Department of Neurology, Tokai University School of Medicine, 143 Shimokasuya, Isehara, Kanagawa 259-1193, Japan
TEL: +81-463-93-1121 (ext. 2242); FAX: +81-463-92-6299; e-mail: enagata@is.icc.u-tokai.ac.jp

Abstract

Although *myo*-inositol pyrophosphates such as diphosphoinositol pentakisphosphate ($InsP_7$) are important in biology, little quantitative mammalian information is available due to the technical difficulty of accurately detecting these materials in biological samples. We have developed an analytical method whereby $InsP_7$ and its precursor inositol hexakisphosphate ($InsP_6$) are determined directly and sensitively using tandem mass spectrometry coupled with hydrophilic interaction liquid chromatography (HILIC). $InsP_6$/$InsP_7$ peak symmetry is greatly influenced by the buffer salt composition and pH of the mobile phase in HILIC analysis. Use of 300 mM ammonium carbonate (pH 10.5) as an aqueous mobile phase resolves each $InsP_6$/$InsP_7$ on a polymer-based amino HILIC column with minimal peak tailing. Method validation shows that $InsP_6$/$InsP_7$ can be quantitated from 20–500 pmol with minimal intra-day/inter-day variance in peak area and retention time. $InsP_6$ concentration in C57BL/6J mouse brain (40.68 ± 3.84 pmol/mg wet weight) was determined using the method. HILIC-MS/MS analysis using HEK293 culture cells confirmed previous observations that $InsP_7$ is induced by NaF treatment and ectopic expression of $InsP_6K2$, a primary kinase for $InsP_7$ synthesis. We have demonstrated that HILIC-MS/MS analysis can quantitate endogenous $InsP_6$/$InsP_7$ in mouse and human samples and expect that the method will contribute to further understanding of $InsP_7$ functions in mammalian pathophysiology.

Keywords:

Inositol polyphosphate

Inositol hexakisphosphate

Diphosphoinositol pentakisphosphate

Hydrophilic interaction liquid chromatography

Tandem mass spectrometry

1. Introduction

Myo-inositol phosphates (hereafter InsPs) occur ubiquitously in animal and plant tissues and play a variety of physiological roles including phosphate storage and signal transduction [1,2]. Inositol hexakisphosphate ($InsP_6$) is the most abundant inositol polyphosphate in mammalian cells and is a precursor of inositol pyrophosphates including diphosphoinositol pentakisphosphate ($InsP_7$). Among three $InsP_6$ kinases ($InsP_6Ks$) present in the mammalian genome, $InsP_6K1$ and $InsP_6K2$ are primarily responsible for the generation of $InsP_7$ [3,4]. This inositol pyrophosphate triggers physiological responses that include gene repair [5], tumor growth/metastasis [6], and neurodegenerative disorders [7-9]. Although inositol pyrophosphates were originally discovered two decades ago [10,11], a complete description of their roles remains elusive due to the lack of direct and sensitive methods to confirm their presence in biological samples.

Many laboratories have developed analytical procedures to detect and quantitate inositol phosphates. Sensitive and selective methods are required, because mammalian specimens contain small amounts of InsPs within a complex biological matrix. In early studies, indirect analyses using radioisotope labeling [12,13] or derivatization [14] were used to determine InsPs abundances in mammalian tissues and cells. Radioisotopic detection coupled with ion exchange chromatography has been a powerful approach for the simultaneous detection of radiolabeled inositol poly/pyrophosphates including $InsP_6$/$InsP_7$, which are synthesized by incorporating [^{3}H]inositol into the inositol phosphate metabolism of cultured cells. Despite the availability of these approaches, indirect analyses have drawbacks of inconsistent labeling efficiency, use of radioactive material and limited applicability to different sample types. Subsequently, a number of

79 sensitive LC-MS(/MS)-based methods that do not require pretreatment have been
80 reported in response to the urgent demand for direct analysis of InsPs. Two research
81 groups have reported reverse phase LC-MS(/MS) assays using ion-pairing agents for
82 $InsP_6$ detection in biological fluids [15,16]. Other groups have advocated ion
83 chromatography-MS(/MS) analysis for quantitative detection of inositol phosphates in
84 various biological samples [17-19]. Although these LC-MS(/MS) procedures afford
85 direct measurement of $InsP_6$ and lower InsPs including $InsP_3$, LC-MS(/MS) methods for
86 detection of higher InsPs such as $InsP_7$ have not been developed.
87 In this study, we describe a sensitive and robust LC-MS/MS method for simultaneous
88 measurement of $InsP_7$ and its precursor $InsP_6$ in mouse and human tissue and cell line
89 using hydrophilic interaction liquid chromatography (HILIC), which provides
90 chromatographic separation of polar molecules and is compatible with MS detection
91 [20,21]. We seek to optimize the MS and HILIC conditions to achieve optimal
92 sensitivity and adequate chromatographic separation. Using HILIC-MS/MS, we are able
93 to confirm the presence or absence of $InsP_7$ and $InsP_6$ and determine their
94 concentrations with high accuracy in mouse brain and human culture cells.
95
96

2. Materials and Methods

2.1. Reagents and materials

LC-MS grade acetonitrile and ammonium bicarbonate were purchased from Honeywell Burdick & Jackson (Morristown, NJ, USA). Ultrapure water was obtained from Wako Pure Chemical Industries (Osaka, Japan). Ultrapure-grade ammonium hydroxide (28% w/v) was obtained from Kanto Chemical (Tokyo, Japan). $InsP_6$, ammonium formate, and ammonium acetate were purchased from Sigma-Aldrich (St. Louis, MO, USA). Hexadeutero-*myo*-inositol trispyrophosphate (ITPP-d_6) was purchased from Toronto Research Chemicals (North York, Canada). $InsP_7$ was synthesized from *myo*-inositol using fluorenylmethyl phosphoramidite chemistry as previously described [22].

2.2. LC separation and chromatographic mobile phase

Chromatographic separation was achieved with an UHPLC-Nexera system (Shimadzu, Kyoto, Japan). Hydrophilic interaction liquid chromatography was performed using a 2.0 × 150 mm, 5-μm HILICpak VG-50 column (Shodex, Tokyo, Japan). This analytical column is made of a polymer-based packing material, which allows chromatographic separations to be performed under strongly alkaline conditions. The column temperature was 45 °C. Optimal aqueous mobile phase conditions (eluent A) were determined by surveying different concentrations (100, 200, 250, 300, and 350 mM) and pH values (9.0, 9.5, 10.0, 10.5, and 11.0) of ammonium carbonate buffer and 300 mM ammonium formate or ammonium acetate buffer at pH 10.0. Buffer pH was adjusted by addition of ammonium hydroxide. Acetonitrile was used as the organic mobile phase (eluent B) at a flow rate of 0.4 mL/min. Linear gradient separation using

ammonium carbonate buffer was achieved by varying the concentrations of the aqueous and organic phases as follows: 0 to 2 min, 65% B; 2 to 12 min, 65 → 2% B; 12 to 15 min, 2% B. The gradient was then restored to the initial composition (65% B), and the column was equilibrated for 15 min before the next run. Linear gradient separations using ammonium formate or ammonium acetate buffers as aqueous eluents were carried out by the same protocol, but with an initial and final ratio of 50% B. The peak symmetry of each analyte was established in terms of the tailing factor (TF), which was calculated at 5% of the peak height according to [23].

2.3. Instrumental analysis

Mass spectrometric analysis was performed by use of an LCMS-8050 triple quadrupole mass spectrometer (Shimadzu, Kyoto, Japan). The ESI ion source was operated in the negative ion mode for detection of each analyte. Ion source settings for the interface, desolvation line, and heat block temperatures were 300, 250, and 400 °C, respectively. The nebulizer, heating, and drying gas flow rates were 3, 10, and 10 L/min, respectively. The ion spray voltage was 3 kV. The resolution for ion selection at Q1 and Q3 were set to unit mass. Data were processed using the Labsolution (version 5.91) software. Mass spectra of precursors and their fragments were obtained by scanning each analyte independently with MS1 or in the product ion scan mode. The selected reaction monitoring (SRM) mode was used to quantitate each analyte. The SRM transitions, collision energies, and other parameters for InsP determinations were optimized based on the greatest sensitivity achieved by flow injecting standards into the MS analyzer. The dwell time for each transition was 80 msec.

2.4. Method validation

The following parameters were assessed for method validation: lower limit of detection (LLOD), lower limit of quantitation (LLOQ), linearity, and precision. Calibration standards of each analyte were prepared in 65:35 acetonitrile:water (v/v) beginning at the LLOD level. The linearity for each analyte was evaluated by calculating the regression coefficient (R^2). LLOD and LLOQ were calculated based on signal-to-noise (S/N) ratios of 3 and 10, respectively. Precision was evaluated in terms of repeatability (intra-day) and reproducibility (inter-day). Repeatability was determined by analyzing three different concentrations of each analyte and calculating the relative standard deviation (RSD) of the retention time and peak area. Reproducibility was determined by injecting the analytes used in the repeatability studies on three different days.

2.5. Mouse and tissue sample preparation

C57 BL/6 mice were maintained in accordance with institutional animal care guidelines (Tokai University School of Medicine). Eight-week old mice were sacrificed to harvest their brains. The brains were rinsed with phosphate-buffered saline and frozen until further use. Frozen brains were homogenized with a Dounce homogenizer in 250 μL ultrapure water. One nmol of ITPP-d_6 was added to the crude lysate as an internal control (IC). Crude lysate was incubated with 125 μL 2 M perchloric acid on ice for 30 min, and the tissue debris was removed by centrifugation. Clear lysates were treated with 400 μL 1 M ammonium acetate, diluted to six-fold volume with ultrapure water, and adjusted to pH 4 with 10% ammonium hydroxide. After centrifugation, lysates were placed on an Oasis WAX anion exchange column (Waters Inc., Milford, MA, USA) and

169 equilibrated with 1 mL 50% MeOH/ultrapure water. The column was rinsed with 1 mL
170 50% MeOH/ultrapure water, and the sample was eluted with 1 mL 1 M ammonium
171 formate. Eluted samples were mixed with acetonitrile to achieve a final concentration of
172 20% MeCN. 50 μL of the mixture was injected into the LC-MS.
173
174 **2.6. Cell culture, treatments, and sample preparation with titanium dioxide beads**
175 HEK293 cells were cultured in DMEM (Nacalai Tesque, Kyoto, Japan) supplemented
176 with 10% FBS in 5% CO_2. Cells prepared at 60% confluence in 10-cm dishes were
177 either treated with 50 mM sodium fluoride (Sigma-Aldrich) for 1 h or subjected to
178 transfection of pEGFP-InsP_6K2 or its empty vector pEGFP-C1 plasmid by
179 polyethyleneimine "Max" reagent (Polysciences, Inc., Warrington, PA) one day before
180 harvesting. Cells were washed twice in PBS and lysed with cell lysis buffer (0.01%
181 Triton X-100, 1 mM EDTA, 20 mM Tris-HCl). A small aliquot was set aside for protein
182 quantitation and subsequent Western blot analysis. Purification of both InsPs with
183 titanium dioxide (TiO_2) beads was carried out with minor modification of a recently
184 described procedure [24]. A half-volume of 2 M perchloric acid (PCA) was added in the
185 cell lysate. After spiking with 1 nmol ITPP-d_6 as an IC, 5 mg of TiO_2 beads were mixed
186 in each sample. The beads were incubated at 4 °C for 30 min and washed twice in PCA.
187 200 μL 10% ammonium hydroxide was added to the beads to elute the InsPs, and the
188 elution step was repeated for maximum recovery. The total eluate was dried using a
189 SpeedVac concentrator (Thermo Scientific, Waltham, MA, USA) and reconstituted in
190 500 μL 100 mM ammonium carbonate/40% MeCN buffer, of which 50 μL was applied
191 to LC-MS.
192

193 **2.7. Western blot**

194 Western blot analysis was performed as previously described [25]. Membranes were
195 incubated with anti-GFP (MBL, Nagoya, Japan) and β-actin (Sigma-Aldrich) primary
196 antibodies overnight at 4 °C. Immunoreactivities of primary antibodies were visualized
197 with Immobilon-Western Chemiluminescent HRP Substrate (Millipore, Billerica, MA,
198 USA) and recorded using an Ez-Capture Analyzer (ATTO, Tokyo, Japan).

199

200 **2.8. Statistical analysis**

201 Data are expressed as mean ± SD. Statistical analysis was performed by one-way
202 analysis of variance (ANOVA) followed by the Bonferroni-type post hoc test.

203

204

205 **3. Results and Discussion**

206 **3.1. MS/MS fragments and optimal SRM parameters for $InsP_6$/$InsP_7$ and internal**
207 **control ITPP-d_6**

208 To understand the mass spectrometric ionization and fragmentation of $InsP_6$/$InsP_7$,
209 their precursor and product ion spectra were obtained by injecting standards into a
210 tandem mass spectrometer. MS1 ion scanning of $InsP_6$ detected its $[M-H]^-$ (*m/z* 658.90)
211 and $[M-2H]^{2-}$ (*m/z* 329.00) precursor ions (Fig. 1A). MS/MS fragmentation of singly
212 and doubly deprotonated $InsP_6$ precursors produced a series of characteristic fragments
213 corresponding to loss of H_2O (18 Da) and/or HPO_3 (80 Da) (Fig. 1B). The spectrum of
214 $InsP_7$ contained its $[M-H]^-$ (*m/z* 739.00) and $[M-2H]^{2-}$ (*m/z* 369.00) precursor ions,
215 although the signal of the singly deprotonated form was weak (Fig 1C). $InsP_6$ detected
216 in the synthetic $InsP_7$ standard is an impurity as a result of $InsP_7$ hydrolysis. The gel
217 electrophoretic image and ^{31}P-NMR spectrum of synthetic $InsP_7$ standard enabled
218 quantitation of the $InsP_6$ impurity (ca. 12%) in the $InsP_7$ standard (Supplementary Fig.
219 1). MS/MS fragmentation of the singly and doubly deprotonated $InsP_7$ precursors
220 produced patterns similar to those of the $InsP_6$ precursors (Fig. 1D). ITPP-d_6 was used
221 as an internal control, because it is commercially available and structurally similar to
222 $InsP_6$/$InsP_7$. Product ion scanning of ITPP-d_6 precursors ($[M-H]^-$, *m/z* 611.00, $[M-2H]^{2-}$,
223 *m/z* 305.00) produced fragments corresponding to loss of water and/or phosphate
224 molecules as with $InsP_6$/$InsP_7$ (Supplementary Fig. 2). Thus, $InsP_6$/$InsP_7$ and ITPP-d_6
225 precursor ions are detected primarily in their singly and doubly deprotonated forms.
226 Collision-induced dissociation preferentially removes water molecules and phosphate
227 moieties covalently linked to the inositol ring.

228 MS source parameters were optimized to maximize the sensitivity of SRM detection.

The most easily detected SRM transitions in Table 1 for $InsP_6$, $InsP_7$, and ITPP-d_6 were *m/z* 658.90 > 561.00, *m/z* 369.00 > 319.95, and *m/z* 305.00 > 78.90, respectively. Given the InsP fragmentation patterns, product ions at *m/z* 561.00 ($InsP_6$), 319.95 ($InsP_7$), and 78.90 (ITPP-d_6) are assigned to $[M\text{-}HPO_3\text{-}H_2O\text{-}H]^-$, $[M\text{-}HPO_3\text{-}H_2O\text{-}2H]^{2-}$, and $[PO_3]^-$, respectively. The most intense SRM transitions were used for quantitative analysis; the remaining transitions were used for identification.

3.2. Aqueous mobile phase for efficient chromatographic separation of $InsP_6$/$InsP_7$

The highly polar nature of the phosphoric acid group complicates the chromatographic separation of phosphate compounds by interacting electrostatically with metal ions on the inner wall of the stainless steel tube and capillary sprayer. This property results in severe peak tailing [26,27]. Asakawa et al. reported that a carbonate modifier and an extremely alkaline aqueous mobile phase mitigate the severe peak tailing of phosphate compounds such as nucleotide phosphates by suppressing their interaction with metal ions [28]. Thus, we used ammonium carbonate buffer as an aqueous mobile phase and acetonitrile (a conventional organic sorbent for HILIC analysis) as an organic mobile phase and sought to determine a suitable ammonium carbonate concentration to minimize $InsP_6$/$InsP_7$ peak tailing in HILIC separations on a polymer-based amino column (Fig. 2A). We used different concentrations of ammonium carbonate buffer in strongly alkaline solution (pH 10.0) to circumvent the effect of pH on peak tailing. 100–300 mM ammonium carbonate decreased $InsP_6$ and $InsP_7$ peak tailing in a concentration dependent manner. Further increases in ammonium carbonate concentration offered little improvement, which indicates that 300 mM is optimal for peak tailing reduction. The same concentration of ammonium acetate or ammonium

253 formate did not improve peak shapes consistent with a previous report that these anions
254 have minimal impact on the peak tailing of phosphate compounds [28]. The effect of
255 aqueous mobile phase pH on peak tailing was investigated in 300 mM ammonium
256 carbonate buffer at pH 9.0–11.0 (Fig. 2B). Maximum suppression occurred at pH 10.5.
257 Thus, $InsP_6$, $InsP_7$, and ITPP-d_6 SRM peaks with acceptable tailing were observed with
258 ammonium carbonate (pH 10.5) mobile phase (Fig. 2C). The retention time of $InsP_6$,
259 $InsP_7$, and ITPP-d6 were 5.8, 6.1, and 4.5 min, respectively. Thus, 300 mM ammonium
260 carbonate pH 10.5 and acetonitrile were determined to be suitable mobile phases for
261 $InsP_6$/$InsP_7$ HILIC analysis.

262 Baseline resolution of $InsP_6$ and $InsP_7$ was not achieved under these chromatographic
263 conditions, although each SRM peak was visibly detectable. McIntyre et al. pointed out
264 that in-source fragmentation of higher InsPs produces fragment ions isobaric with lower
265 InsPs and thereby can cause errors in quantitating lower InsPs [29]. We did not observe
266 $InsP_6$ peak co-chromatographed with $InsP_7$, which implies that minimal isobaric $InsP_6$
267 fragments are produced by $InsP_7$ decomposition at the ESI ion source. Thus, the
268 influence of in-source $InsP_7$ fragmentation on $InsP_6$ quantitation is limited under our
269 analytical conditions. However, further exploration of chromatographic conditions
270 providing complete separation of $InsP_7$ and $InsP_6$ SRM peaks may be needed to
271 establish reliable quantitative analysis. Factors inducing in-source fragmentation of
272 $InsP_7$ should be avoided for accurate quantitation as long as $InsP_6$ and $InsP_7$ are not fully
273 resolved.

274

275 **3.3. Method validation**

276 The calibration curve linearity, retention time and peak area precision, and lower limit

277 of detection (LLOD) and quantitation (LLOQ) were evaluated with corresponding
278 standards to validate the sensitivity and robustness of the LC-MS/MS method (Table 2).
279 Linearity was evaluated over concentrations ranging from the LLOD to the highest
280 calibration point (500 pmol) using the external quantitation method. Linear calibration
281 curves were observed for $InsP_6$, $InsP_7$, and ITPP-d_6 over the entire concentration range.
282 The linear regression coefficient (R^2) was greater than 0.99 for all analytes. Intra- and
283 inter-day variations in retention time were less than 7%, and peak area variations were
284 less than 16%. The LLOD was 5 pmol, 2 pmol, and 20 fmol for $InsP_6$, $InsP_7$, and
285 ITPP-d_6, respectively, and the LLOQ was 20 pmol for $InsP_6$ and $InsP_7$ and 50 fmol for
286 ITPP-d_6. These sensitivities are comparable to those of a previously reported LC-MS
287 method for $InsP_6$ quantitation [15]. Thus, our LC-MS/MS method provides a sensitive
288 and robust determination of $InsP_6$/$InsP_7$ concentrations at the picomole level.
289
290 **3.4. Absolute abundance of endogenous $InsP_6$/$InsP_7$ in mouse brain and human**
291 **culture cells**
292 We assessed the applicability of HILIC-MS/MS to the quantitative analysis of
293 mammalian-derived $InsP_6$/$InsP_7$ by examining the endogenous $InsP_6$/$InsP_7$ content in
294 C57BL/6J mouse brain. Fig. 3A shows SRM chromatograms of non-spiked mouse brain
295 samples and those spiked with $InsP_6$/$InsP_7$ before sample preparation. The prominent
296 $InsP_6$ peak in the non-spiked sample has the same retention time as the $InsP_6$ peak of the
297 $InsP_6$/$InsP_7$-spiked sample. Quantitative analysis reveals that the presence of 40.68±3.84
298 pmol/mg wet weight $InsP_6$ in normal C57BL/6J mouse brain. This value is roughly
299 comparable to the $InsP_6$ concentration in rat brain (194.7±25.5 pmol/mg of protein),
300 which was measured by in vitro $InsP_6$ phosphorylation with [γ-^{32}P]ATP [30]. In contrast

301 to $InsP_6$, endogenous $InsP_7$ was not detected in mouse brain. In light of previous reports
302 that $InsP_6$ kinase activity is triggered by various stresses and thereby dormant in normal
303 circumstances [31], it is reasonable to assume that the $InsP_7$ level is negligible in normal
304 mouse brain. $InsP_7$ is induced by NaF treatment of mammalian cells, which is attributed
305 to the inhibitory action of fluoride ion on intracellular pyrophosphatase activity [10].
306 Our observations using HEK293 cells show that NaF treatment causes a significant
307 increase in the $InsP_7$ level (11.10±2.20 vs. 1047.16±171.98 pmol/mg protein, $P < 0.05$)
308 accompanied by a small decrease in $InsP_6$ (2.84±0.57 vs. 2.00±0.50 nmol/mg protein, P
309 = 0.057) (Fig. 3B and C). The increase in $InsP_7$ is almost equivalent to the extent of
310 $InsP_6$ reduction in NaF-treated cells, which is consistent with the view that the
311 intracellular $InsP_6$ pool is a dominant source of $InsP_7$ production [32]. We also utilized
312 HILIC-MS/MS to investigate the $InsP_7$ level in $InsP_6$K2-overexpressing cells (Fig. 3E).
313 The analysis reveals that $InsP_6$K2 ectopic expression produces an approximately 10-fold
314 enhancement of $InsP_7$ induction over the vector control (Fig. 3D and F). In summary,
315 our HILIC-MS/MS method is applicable to the quantitative analysis of mouse- and
316 human-derived $InsP_6$/$InsP_7$.
317
318

4. Conclusion

We have developed a novel HILIC-MS/MS method for separating and quantitating $InsP_7$ and its $InsP_6$ precursor. This sensitive and direct method of $InsP_7$ analysis is notable, because previous methods have required radioisotope labelling with ^{3}H or ^{32}P, and no LC-MS assays for $InsP_7$ have been reported. MS parameters and LC conditions were refined to establish the greatest sensitivity of detection and optimum chromatographic behavior on a polymer-based amino HILIC column. The HILIC-MS/MS method enables the simultaneous quantitation of $InsP_6$/$InsP_7$ at the picomole level in a single chromatographic run of 30 min. Using this analytical procedure, we have successfully determined the absolute concentration of endogenous $InsP_6$/$InsP_7$ in mouse brain and human cultured cells. We are confident that this HILIC-MS/MS method will provide new insights into the pathogenic role of inositol pyrophosphate by facilitating in-depth investigations of cancer and various neurodegenerative disorders.

Acknowledgment

The technical advice of Dr. Junji Sasuga at Shodex is greatly acknowledged. We also appreciate Drs. Shunji Kato and Hisako Akatsuka for critical reading of the manuscript, and Editage (www.editage.jp) for English language editing. This research did not receive any specific grant from funding agencies in the public, commercial, or not-for-profit sectors.

343 **References**

344 [1] S.K. Fisher, J.E. Novak, B.W. Agranoff, Inositol and higher inositol phosphates in
345 neural tissues: homeostasis, metabolism and functional significance, J. Neurochem. 82
346 (2002) 736-754.
347 [2] A. Saiardi, How inositol pyrophosphates control cellular phosphate homeostasis?
348 Adv. Biol. Regul. 52 (2012) 351-359.
349 [3] E. Nagata, H.R. Luo, A. Saiardi, B.I. Bae, N. Suzuki, S.H. Snyder, Inositol
350 hexakisphosphate kinase-2, a physiologic mediator of cell death, J. Biol. Chem. 280
351 (2005) 1634-1640.
352 [4] M.A. Koldobskiy, A. Chakraborty, J.K. Werner Jr, A.M. Snowman, K.R. Juluri,
353 M.S. Vandiver, S. Kim, S. Heletz, S.H. Snyder, P53-Mediated Apoptosis Requires
354 Inositol Hexakisphosphate Kinase-2, Proc. Natl. Acad. Sci. U. S. A. 107 (2010)
355 20947-20951.
356 [5] F. Rao, J. Xu, A.B. Khan, M.M. Gadalla, J.Y. Cha, R. Xu, R. Tyagi, Y. Dang, A.
357 Chakraborty, S.H. Snyder, Inositol hexakisphosphate kinase-1 mediates
358 assembly/disassembly of the CRL4-signalosome complex to regulate DNA repair and
359 cell death, Proc. Natl. Acad. Sci. U. S. A. 111 (2014) 16005-16010.
360 [6] F. Rao, J. Xu, C. Fu, J.Y. Cha, M.M. Gadalla, R. Xu, J.C. Barrow, S.H. Snyder,
361 Inositol pyrophosphates promote tumor growth and metastasis by antagonizing liver
362 kinase B1, Proc. Natl. Acad. Sci. U. S. A. 112 (2015) 1773-1778.
363 [7] E. Nagata, A. Saiardi, H. Tsukamoto, Y. Okada, Y. Itoh, T. Satoh, J. Itoh, R.L.
364 Margolis, S. Takizawa, A. Sawa, S. Takagi, Inositol hexakisphosphate kinases induce
365 cell death in Huntington disease, J. Biol. Chem. 286 (2011) 26680-26686.

366 [8] C. Fu, J. Xu, R.J. Li, J.A. Crawford, A.B. Khan, T.M. Ma, J.Y. Cha, A.M. Snowman,
367 M.V. Pletnikov, S.H. Snyder, Inositol Hexakisphosphate Kinase-3 Regulates the
368 Morphology and Synapse Formation of Cerebellar Purkinje Cells via Spectrin/Adducin,
369 J. Neurosci. 35 (2015) 11056-11067.
370 [9] E. Nagata, T. Nonaka, Y. Moriya, N. Fujii, Y. Okada, H. Tsukamoto, J. Itoh, C.
371 Okada, T. Satoh, T. Arai, M. Hasegawa, S. Takizawa, Inositol Hexakisphosphate
372 Kinase 2 Promotes Cell Death in Cells with Cytoplasmic TDP-43 Aggregation, Mol.
373 Neurobiol. 53 (2016) 5377-5383.
374 [10] F.S. Menniti, R.N. Miller, J.W. Putney Jr, S.B. Shears, Turnover of inositol
375 polyphosphate pyrophosphates in pancreatoma cells, J. Biol. Chem. 268 (1993)
376 3850-3856.
377 [11] L. Stephens, T. Radenberg, U. Thiel, G. Vogel, K.H. Khoo, A. Dell, T.R. Jackson,
378 P.T. Hawkins, G.W. Mayr, The detection, purification, structural characterization, and
379 metabolism of diphosphoinositol pentakisphosphate(s) and bisdiphosphoinositol
380 tetrakisphosphate(s), J. Biol. Chem. 268 (1993) 4009-4015.
381 [12] L.R. Stephens, C.P. Downes, Product-precursor relationships amongst inositol
382 polyphosphates. Incorporation of [32P]Pi into myo-inositol 1,3,4,6-tetrakisphosphate,
383 myo-inositol 1,3,4,5-tetrakisphosphate, myo-inositol 3,4,5,6-tetrakisphosphate and
384 myo-inositol 1,3,4,5,6-pentakisphosphate in intact avian erythrocytes, Biochem. J. 265
385 (1990) 435-452.
386 [13] C. Azevedo, A. Saiardi, Extraction and analysis of soluble inositol polyphosphates
387 from yeast, Nat. Protoc. 1 (2006) 2416-2422.

[14] J.G. March, B.M. Simonet, F. Grases, Determination of phytic acid by gas chromatography-mass spectroscopy: application to biological samples, J. Chromatogr. B Biomed. Sci. Appl. 757 (2001) 247-255.

[15] F. Tur, E. Tur, I. Lentheric, P. Mendoza, M. Encabo, B. Isern, F. Grases, C. Maraschiello, J. Perello, Validation of an LC-MS bioanalytical method for quantification of phytate levels in rat, dog and human plasma, J. Chromatogr. B. Analyt Technol. Biomed. Life. Sci. 928 (2013) 146-154.

[16] B. Rougemont, C. Fonbonne, J. Lemoine, B. Vanessa, A. Salvador, Liquid chromatography coupled to tandem mass spectrometry for the analysis of inositol hexakisphosphate after solid phase extraction, J. Liq. Chromatogr. Relat. Technol. 39 (2016) 408-414.

[17] X. Liu, P.W. Villalta, S.J. Sturla, Simultaneous determination of inositol and inositol phosphates in complex biological matrices: quantitative ion-exchange chromatography/tandem mass spectrometry, Rapid Commun. Mass Spectrom. 23 (2009) 705-712.

[18] P.J.R. Sjoberg, P. Thelin, E. Rydin, Separation of inositol phosphate isomers in environmental samples by ion-exchange chromatography coupled with electrospray ionization tandem mass spectrometry, Talanta 161 (2016) 392-397.

[19] Q.H. Duong, K.D. Clark, K.G. Lapsley, R.B. Pegg, Quantification of inositol phosphates in almond meal and almond brown skins by HPLC/ESI/MS, Food Chem. 229 (2017) 84-92.

[20] C. Gorgens, S. Guddat, W. Schanzer, M. Thevis, Screening and confirmation of myo-inositol trispyrophosphate (ITPP) in human urine by hydrophilic interaction liquid

411 chromatography high resolution / high accuracy mass spectrometry for doping control
412 purposes, Drug Test. Anal. 6 (2014) 1102-1107.
413 [21] S. Tufi, M. Lamoree, J. de Boer, P. Leonards, Simultaneous analysis of multiple
414 neurotransmitters by hydrophilic interaction liquid chromatography coupled to tandem
415 mass spectrometry, J. Chromatogr. A 1395 (2015) 79-87.
416 [22] I. Pavlovic, D.T. Thakor, J.R. Vargas, C.J. McKinlay, S. Hauke, P. Anstaett, R.C.
417 Camuna, L. Bigler, G. Gasser, C. Schultz, P.A. Wender, H.J. Jessen, Cellular delivery
418 and photochemical release of a caged inositol-pyrophosphate induces PH-domain
419 translocation *in cellulo*, Nat. Commun. 7 (2016) 10622.
420 [23] Aubin, European Pharmacopoeia (5th ed.). Ligugé, France, 2004, pp. 69-72.
421 [24] M.S. Wilson, S.J. Bulley, F. Pisani, R.F. Irvine, A. Saiardi, A novel method for the
422 purification of inositol phosphates from biological samples reveals that no phytate is
423 present in human plasma or urine, Open Biol. 5 (2015) 150014.
424 [25] N. Yuasa, E. Nagata, N. Fujii, M. Ito, H. Tsukamoto, S. Takizawa, Serum
425 apolipoprotein E may be a novel biomarker of migraine, PLoS One 13 (2018)
426 e0190620.
427 [26] R. Tuytten, F. Lemiere, E. Witters, W. Van Dongen, H. Slegers, R.P. Newton, H.
428 Van Onckelen, E.L. Esmans, Stainless steel electrospray probe: a dead end for
429 phosphorylated organic compounds? J. Chromatogr. A 1104 (2006) 209-221.
430 [27] H. Sakamaki, T. Uchida, L.W. Lim, T. Takeuchi, Evaluation of column hardware
431 on liquid chromatography-mass spectrometry of phosphorylated compounds, J.
432 Chromatogr. A 1381 (2015) 125-131.
433 [28] Y. Asakawa, N. Tokida, C. Ozawa, M. Ishiba, O. Tagaya, N. Asakawa,
434 Suppression effects of carbonate on the interaction between stainless steel and

435 phosphate groups of phosphate compounds in high-performance liquid chromatography
436 and electrospray ionization mass spectrometry, J. Chromatogr. A 1198-1199 (2008)
437 80-86.
438 [29] C.A. McIntyre, C.J. Arthur, R.P. Evershed, High-resolution mass spectrometric
439 analysis of myo-inositol hexakisphosphate using electrospray ionisation Orbitrap, Rapid
440 Commun. Mass Spectrom. 31 (2017) 1681-1689.
441 [30] A.J. Letcher, M.J. Schell, R.F. Irvine, Do mammals make all their own inositol
442 hexakisphosphate? Biochem. J. 416 (2008) 263-270.
443 [31] P.C. Fridy, J.C. Otto, D.E. Dollins, J.D. York, Cloning and characterization of two
444 human VIP1-like inositol hexakisphosphate and diphosphoinositol pentakisphosphate
445 kinases, J. Biol. Chem. 282 (2007) 30754-30762.
446 [32] S. Mulugu, W. Bai, P.C. Fridy, R.J. Bastidas, J.C. Otto, D.E. Dollins, T.A.
447 Haystead, A.A. Ribeiro, J.D. York, A conserved family of enzymes that phosphorylate
448 inositol hexakisphosphate, Science 316 (2007) 106-109.
449
450
451

452 **Figure captions**

453 Fig. 1. Precursor/product ion spectra of $InsP_6/P_7$. Chemical structures (upper) and
454 precursor ion spectra (lower) of $InsP_6$ (A) and $InsP_7$ (C). Product ion mass spectra
455 derived from singly (upper) and doubly (lower) deprotonated precursor ions of $InsP_6$
456 (B) and $InsP_7$ (D).

457

458 Fig. 2. Optimal aqueous mobile phase conditions in HILIC analysis of $InsP_6/P_7$ and
459 ITPP-d_6. Tailing factor of $InsP_6/P_7$ and ITPP-d_6 peaks as a function of (A) different
460 concentrations of ammonium carbonate (100–350 mM), 300 mM ammonium acetate
461 (AA), and 300 mM ammonium formate (AF) and (B) alkaline pH values of 300 mM
462 ammonium carbonate (pH 9.0–11.0). Values represent the mean ± SD of three injections.
463 (C) SRM chromatograms of $InsP_6/P_7$ and ITPP-d_6 using 300 mM ammonium carbonate
464 (pH 10.5) as an aqueous mobile phase of HILIC analysis. 500 pmol of each analyte was
465 injected into LC-MS. The SRM peak of $InsP_6$ (broken line) is overlaid on that of $InsP_7$.

466

467 Fig. 3. Quantitative HILIC-MS/MS analysis of endogenous $InsP_6/P_7$ in mammalian
468 samples. (A) SRM chromatograms of $InsP_6/P_7$ and ITPP-d_6 in non-spiked (upper) or
469 $InsP_6/P_7$-spiked mouse brain sample (lower). (B) SRM chromatograms of $InsP_6/P_7$ and
470 ITPP-d_6 in untreated (left) and NaF-treated HEK293 cells (right). (C) Concentration of
471 endogenous $InsP_6/P_7$ in HEK293 cells with and without NaF treatment. Values represent
472 the mean ± SD of three injections and are expressed as moles per mg of total cell
473 proteins, *$P<0.05$ vs. untreated. (D) SRM chromatograms of $InsP_6/P_7$ and ITPP-d_6 in
474 HEK293 cells transfected with empty vector (Ctrl, left) or $InsP_6K2$ (right). (E)
475 Representative Western blot image of $InsP_6K2$ protein overexpressed in HEK293 cells.

476 β-actin protein was used as a loading control. (F) Ten-fold enhancement of endogenous
477 $InsP_7$ induction in $InsP_6K2$-overexpressing HEK293 cells. Values represent the mean ±
478 SD of three injections and are expressed relative to Ctrl, *P<0.05 vs. Ctrl.
479

Figure 1

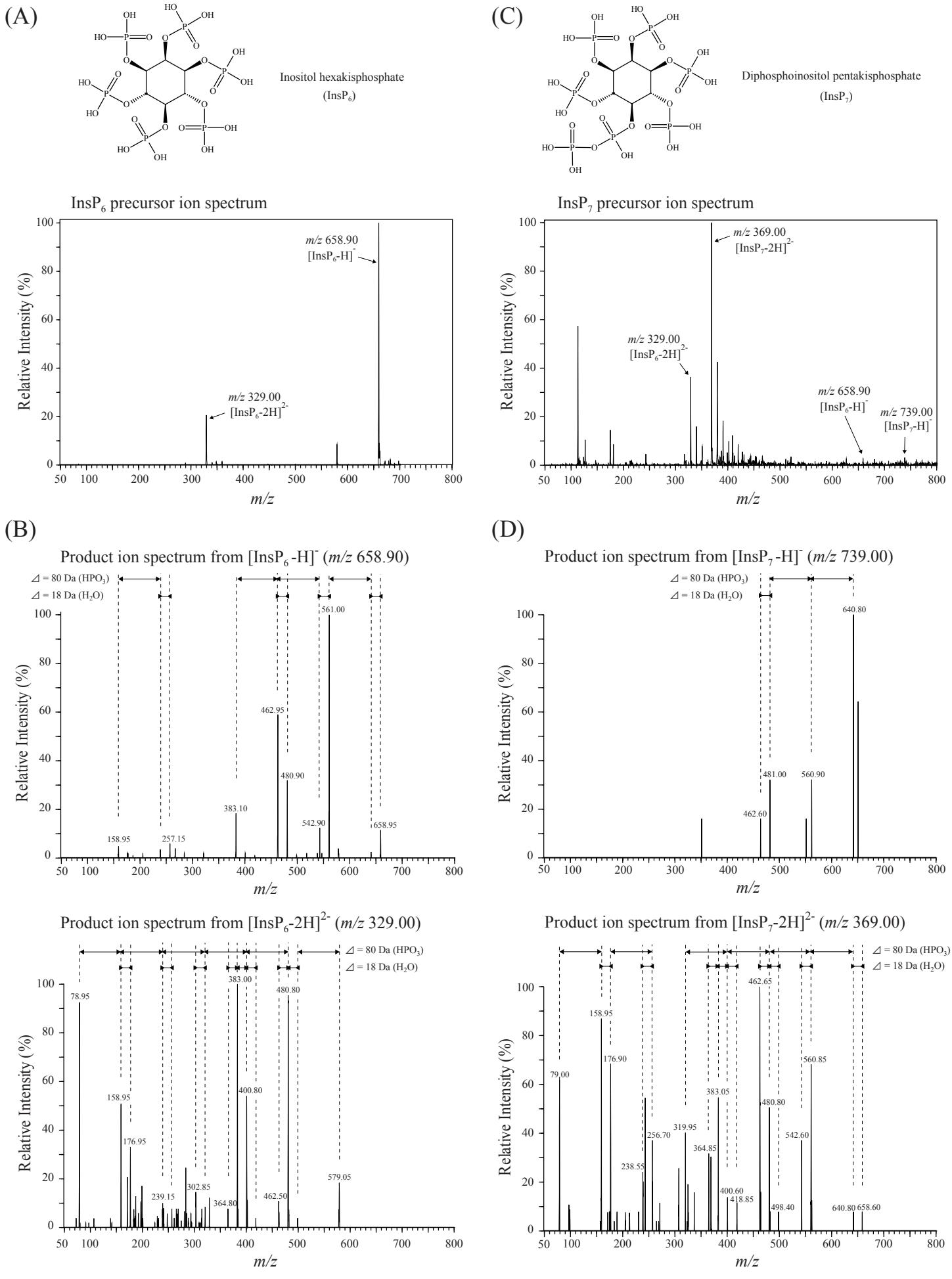

Fig. 1 Ito et al.

Figure 2

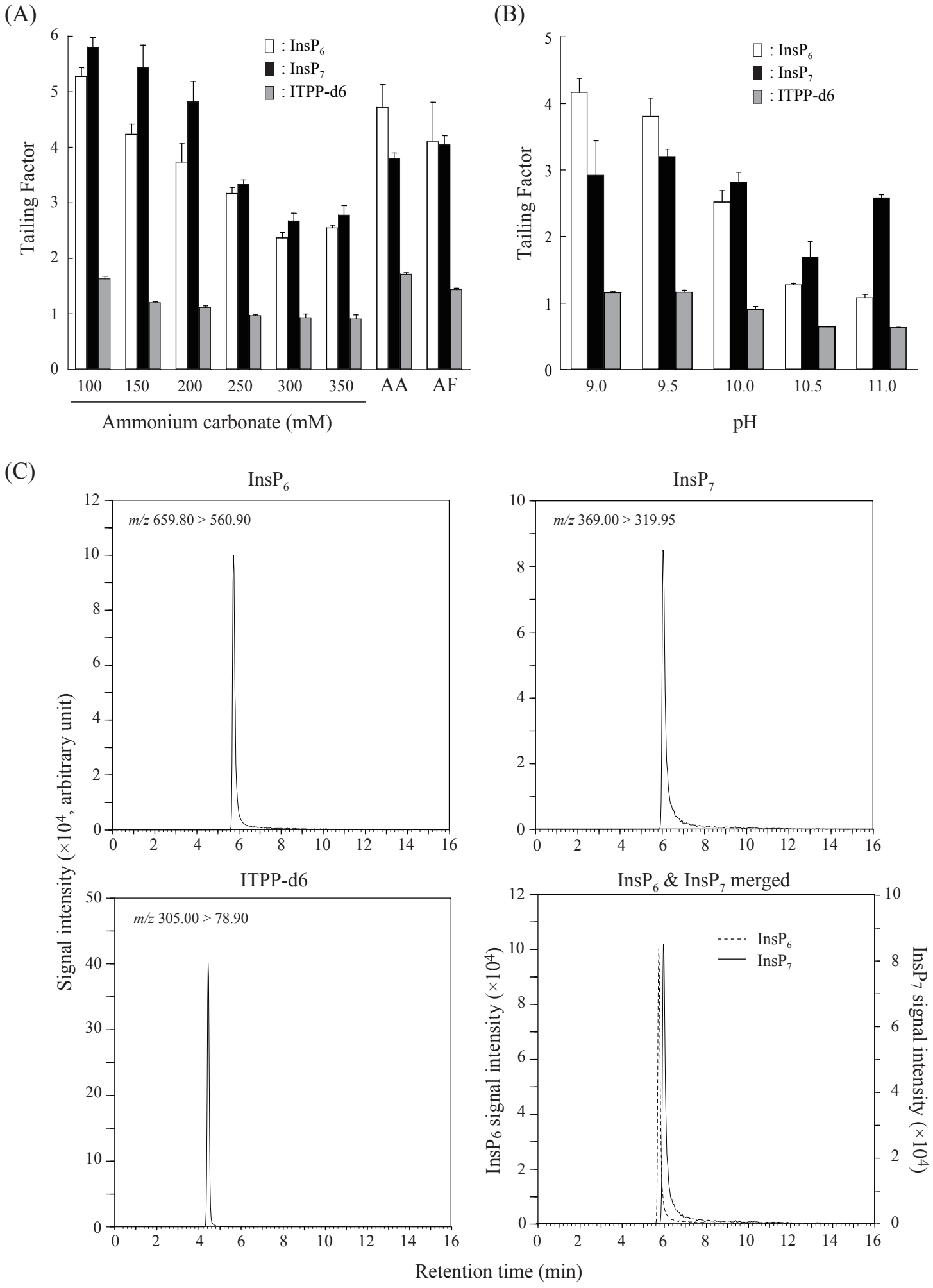

Fig. 2 Ito et al.

Figure 3

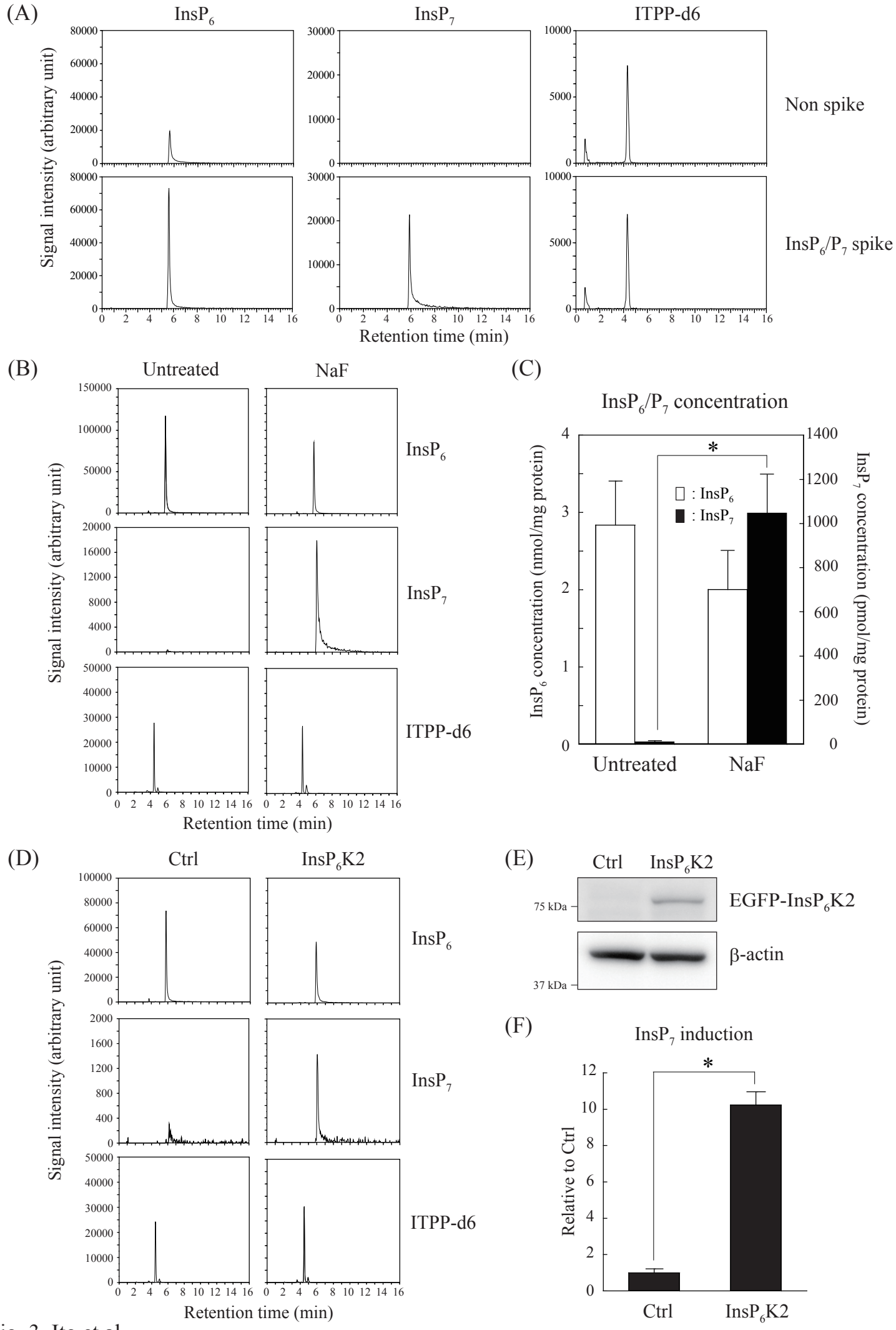

Fig. 3 Ito et al.

Tables

Table 1. Optimized SRM conditions for $InsP_6/P_7$ and ITPP-d_6. Parameters determined by flow injection analysis of 500 pmol of the corresponding standard. Relative intensities are expressed vs. the least sensitive transition of each analyte.

	Transition	Q1pre bias (V)	Collision energy (V)	Q3pre bias (V)	Relative intensity
$InsP_6$	658.90 > 561.00	20	28	26	2.7
	658.90 > 462.95	24	33	14	2.3
	658.90 > 158.95	20	50	25	1.9
	329.00 > 279.95	24	13	11	1.0
	329.00 > 158.95	17	31	28	1.2
	329.00 > 78.95	24	54	17	2.0
$InsP_7$	739.00 > 640.80	38	29	20	1.9
	739.00 > 542.70	26	39	26	1.7
	739.00 > 462.60	28	45	29	1.0
	369.00 > 319.95	26	13	13	6.7
	369.00 > 158.95	13	38	13	2.8
	369.00 > 79.00	14	51	13	4.2
ITPP-d6	611.00 > 530.85	22	31	36	8.2
	611.00 > 450.95	32	40	19	1.6
	611.00 > 158.90	22	55	25	1.0
	305.00 > 158.95	22	31	14	6.3
	305.00 > 78.90	21	44	12	14.2

Table 2. Validation results for quantitation of $InsP_6/P_7$ and ITPP-d_6. Low concentration: 20 pmol, Middle concentration: 100 pmol, High concentration: 500 pmol. Variables x and y in the regression equation denote analyte concentration and peak area, respectively.

	linearity	LLOD (pmol/mL)	LLOQ (pmol/mL)	intra-day precision (%)						inter-day precision (%)					
				peak area			retention time			peak area			retention time		
				Low	Middle	High	Low	Middle	High	Low	Middle	High	Low	Middle	High
$InsP_6$	y=4791x-28064 (R^2=0.9922)	100	400	9.67	2.01	5.69	2.21	0.19	0.20	12.29	12.68	14.94	2.88	0.56	0.51
$InsP_7$	y=2989x-25178 (R^2=0.9953)	40	400	15.05	3.63	3.47	3.25	0.61	0.26	9.80	13.88	3.54	6.52	0.52	0.37
ITPP-d_6	y=9396x+36042 (R^2=0.9977)	0.4	1.0	4.02	3.53	3.48	0.14	0.16	0.12	5.34	5.30	1.68	0.87	0.96	0.77